NANO LETTERS

2007
Vol. 7, No. 1
183−187

Instabilities in Nanoporous Media

Jiun-Tai Chen, Mingfu Zhang, and Thomas P. Russell*

Department of Polymer Science and Engineering, University of Massachusetts, Amherst, Massachusetts 01003

Received September 8, 2006

ABSTRACT

Rayleigh instabilities in thin polymer films confined within nanoporous alumina membranes were studied. Thin films of poly(methyl methacrylate) (PMMA) were prepared by filling cylindrical nanopores in an anodic aluminum oxide (AAO) membrane with a PMMA solution in chloroform followed by solvent evaporation. When the PMMA nanotubes were annealed above the glass transition temperature (T_g), undulations in the film thickness were observed that were induced by a Rayleigh instability. The amplitude of the undulations increased with time and eventually bridged across the cylindrical nanopore in the AAO membrane, resulting in the formation of polymer nanorods with periodic encapsulated holes. A similar behavior was observed when PMMA films were confined within carbon nanotubes (CNTs). The Rayleigh instabilities in these confined geometries offer a novel means of controlling and fabricating the polymer nanostructures. These compartmentalized nanorods may have potential applications as delivery devices.

In recent years, one-dimensional (1-D) nanomaterials including nanotubes, nanowires, and nanorods have attracted significant attention due to their unique properties and many potential applications.[1−4] Although 1-D nanostructures of various materials have been prepared and their properties have been intensively studied, there are still some important issues that need to be addressed, such as their thermal stability.[5,6] Upon thermal annealing, 1-D nanomaterials may have sufficient mobility to undergo structural transformations to minimize the free energy. Molares et al., for example, studied Rayleigh instabilities in copper nanowires at elevated temperatures.[7] After being annealed at elevated temperatures (400−600 °C), much below the melting point of bulk copper (1085 °C), the copper nanowires were found to fragment into chains of nanospheres. One would expect that 1-D polymeric nanomaterials should undergo structure transformations via a similar mechanism when they are heated into the melt state.

Over a century ago, Plateau pioneered the study of instability in liquid cylinders.[8] The instabilities of liquid cylinders arise from surface tension. When the free surface of a liquid cylinder undulates with a wavelength λ, its surface area decreases, as long as λ is greater than the circumference of the cylinder. Subsequently, Rayleigh showed that the instability of a liquid cylinder led to a surface undulation with a well-defined wavelength and, thus, explained the regular spacing of the drops that formed.[9] Similar to liquid cylinders, annular films on fibers or in capillaries also show such instabilities.[10] The observed wavelength corresponds to the fastest growing mode and, for a thin liquid film coated on a fiber of radius b, the wavelength is $\lambda = (2\pi\sqrt{2})b$ when the film thickness $e \ll b$. Rayleigh instabilities also occur when a liquid film is coated onto the wall of a capillary tube. As the amplitude of undulations grows with time and crests may merge to form bridges across the capillary tube, producing a rod with periodic encapsulated holes.[11] Theoretical studies have predicted the formation of such nanorods, but this has not been realized experimentally.[12−14]

Here we use films of poly(methyl methacrylate) (PMMA) coated on the walls of cylindrical nanopores in alumina membranes. These nanotubes of polymer offer a broad range of applications including photonics, sensors, catalysts, and medicine.[15−17] To prepare PMMA nanotubes, we used an anodized aluminum oxide (AAO) membrane as a template. The size of PMMA nanotubes can be easily adjusted by controlling the size of the nanopores within the AAO template which can be controlled by the anodization conditions.[18,19] By using an amorphous, glassy polymer, like PMMA, Rayleigh instabilities can be induced by heating above the glass transition temperature and the resultant nanostructures can be frozen-in simply by quenching to temperatures below the glass transition temperature, T_g. The AAO membrane can be removed easily using a dilute NaOH aqueous solution without perturbing the polymer, so that examination of the resultant polymeric nanostructures is straightforward by transmission electron microscopy (TEM).

As shown in Scheme 1, a four-step process was used to prepare the PMMA nanorods with periodic encapsulated holes. Several drops of 5 wt % PMMA solution in chloroform were placed onto a glass substrate. An AAO membrane was immediately placed on top of the solution and the

* To whom correspondence should be addressed. E-mail: russell@mail.pse.umass.edu. Telephone: +1 (413) 577-1516. Fax: +1 (413) 577-1510.

10.1021/nl0621241 CCC: $37.00
Published on Web 01/10/2007

Scheme 1. Schematic Procedure for the Preparation of PMMA Nanotubes and the Subsequent Structure Transformation Due to the Rayleigh Instability

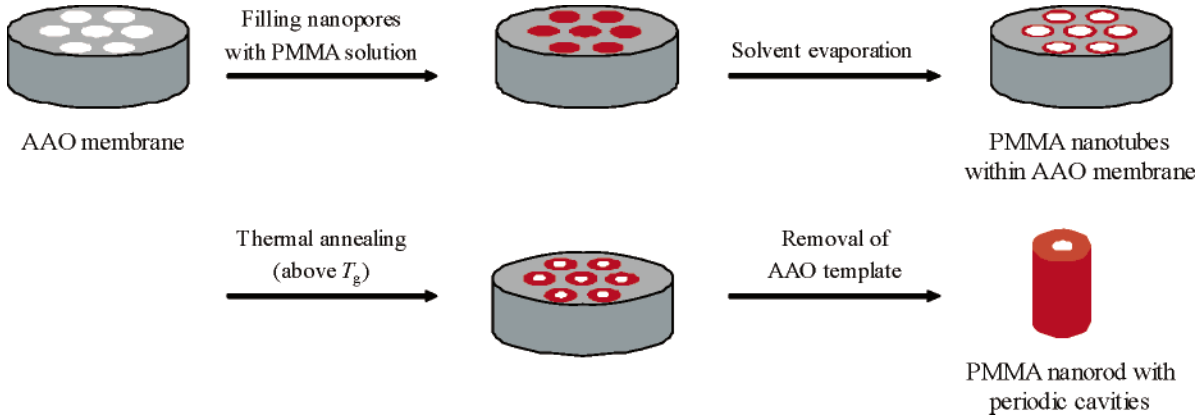

nanopores of the membrane were filled with the PMMA solution within seconds by capillary force.[20] After solvent evaporation at ambient conditions, thin PMMA films were deposited onto the walls of nanopores in the membrane, resulting in the formation of PMMA nanotubes. These nanotubes were further dried at 60 °C under vacuum for 12 h to remove the residual solvent. The Rayleigh instabilities were induced when the sample (AAO coated with PMMA nanotubes) was annealed in vacuum oven at temperatures ranging from 150 to 200 °C for a predetermined period of time, following by a rapid quenching to room temperature. The AAO template was then dissolved using 5 wt % $NaOH_{(aq)}$ and the final PMMA nanostructures were released. The PMMA nanostructures before and after thermal annealing were examined by scanning electron microscopy (SEM) and TEM.

Shown in Figure 1a is an SEM image of bundles of PMMA nanotubes before thermal annealing. The PMMA nanotubes are straight and the length and diameter of the nanotubes are consistent with the size of cylindrical nanopores in the original AAO template. The tube diameter ranges from 100 to 400 nm and the length is ~60 μm. The tubular nature of the structures is seen from the top view shown in Figure 1b. Unlike our previous work,[21] a thick polymer layer below the AAO membrane was not seen after solvent evaporation. The solvent used in these studies was chloroform, which evaporates very rapidly in the nanopores, causing a continuous filling of the pores with the residual solution on the glass substrate. This continued until all of the solution was drained into the porous membrane. Therefore, the observed wall thickness of the nanotubes is much larger than that expected in the absence of continuous filling, based on the relatively low polymer concentration (5 wt %). Parts c and d of Figure 1 show two typical TEM images of the PMMA nanotubes before thermal annealing. The tubular structure is evident. The walls of the tubes are uniform in thickness and some branches in the nanotubes are seen, which arise from imperfections in the original AAO template.[22] A TEM image of a single PMMA nanotube at a higher magnification is shown in Figure 1d. The wall thickness of this tube is ~75 nm with an outer diameter of ~280 nm.

Upon heating the AAO membrane, with the pore walls coated with PMMA, to temperatures above the glass transition temperature of PMMA (T_g ~ 128 °C, as determined by differential scanning calorimetry), the inner walls of PMMA nanotubes showed undulations that grew in amplitude with time and eventually spanned across the nanotube, forming nanorods with periodic encapsulated holes. Parts a and b of Figure 2 are the SEM images of the hole-containing PMMA nanorods after annealing at 150 °C for 8 h. The annual films surrounding the encapsulated pores are very thin and, in some cases, were broken during sample preparation and/or electron microscopy measurements (beam damage) as one can see

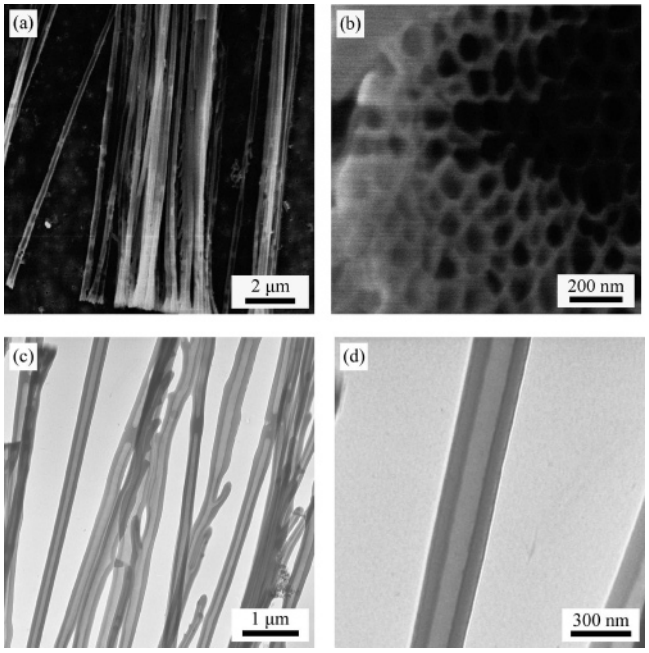

Figure 1. Electron micrographs of PMMA nanotubes prepared using an AAO membrane as a template. The AAO template was removed by 5 wt % $NaOH_{(aq)}$ and PMMA nanorods were then placed on a filter paper for SEM measurements and on a Formvar-coated copper grid for TEM measurements: (a) SEM image of bundles of PMMA nanotubes; (b) SEM image of the top view of bundles of the PMMA nanotubes. The tube ends are all open: (c) lower magnification of TEM image of PMMA nanotubes; (d) higher magnification of TEM image of a single PMMA nanotube.

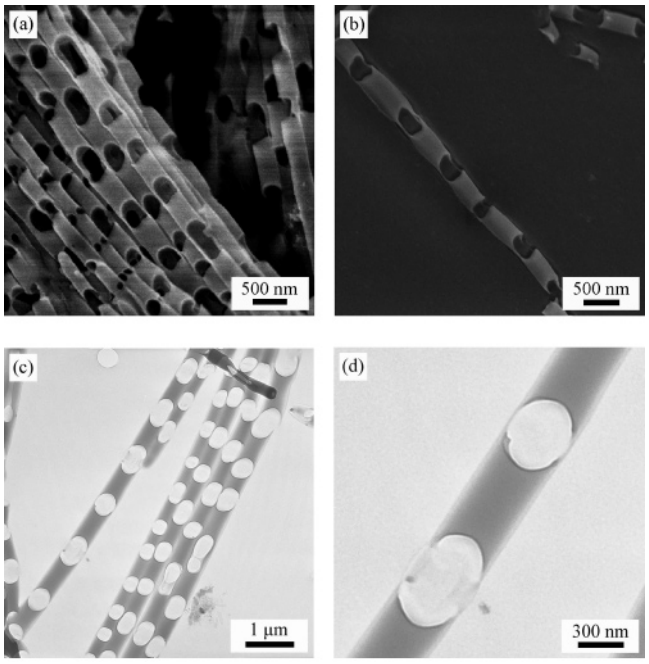

Figure 2. Electron micrographs of hole-containing PMMA nanorods after annealing PMMA nanotubes within an AAO membrane at 150 °C for 8 h: (a) SEM image of bundles of hole-containing PMMA nanorods; (b) SEM image of a single hole-containing PMMA nanorod; (c) TEM image of hole-containing PMMA nanorods with lower magnification; (d) TEM image of a single hole-containing PMMA nanorod with higher magnification.

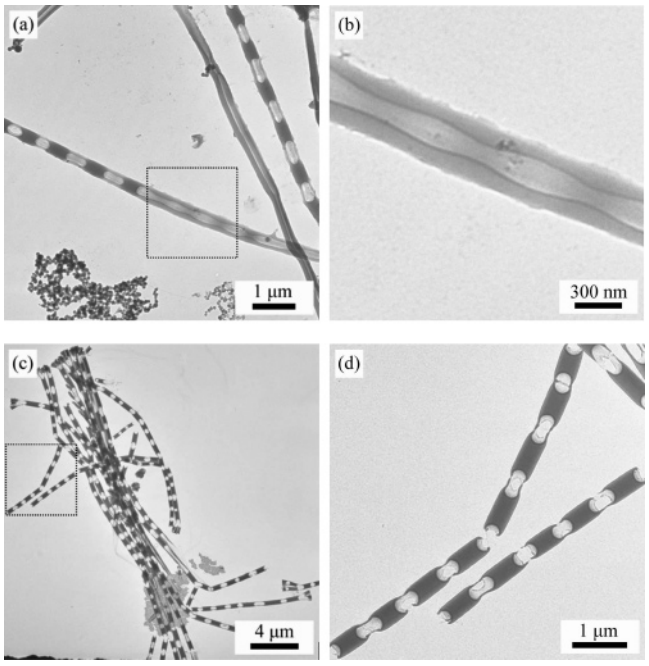

Figure 3. TEM images of hole-containing PMMA nanorods after annealing at 200 °C for different times: (a, b) sample annealed for 10 min, where part b is a magnification of the piece shown in part a marked by the frame; (c, d) sample annealed for 20 min, where part d is a magnification of the piece shown in part c marked by the frame.

from the SEM images. Figure 2b shows a single hole-containing nanorod. TEM images, Figure 2, parts c and d, show structures of the nanorods having regularly spaced

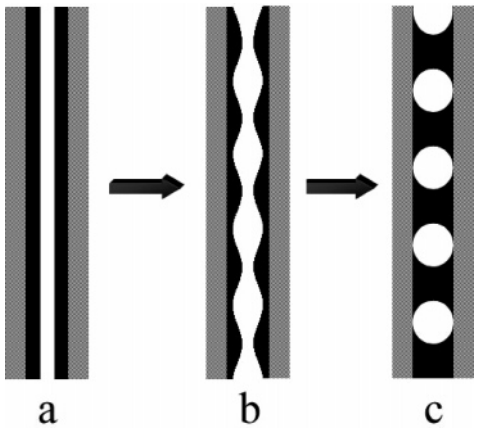

Figure 4. Mechanism of the transformation from a polymer nanotube to a hole-containing polymer nanorod inside the cylindrical nanopore of an AAO template driven by the Rayleigh instability: (a) a polymer nanotube coated on the pore wall in an AAO template; (b) surface undulation of a polymer nanotube; (c) formation of capillary bridges.

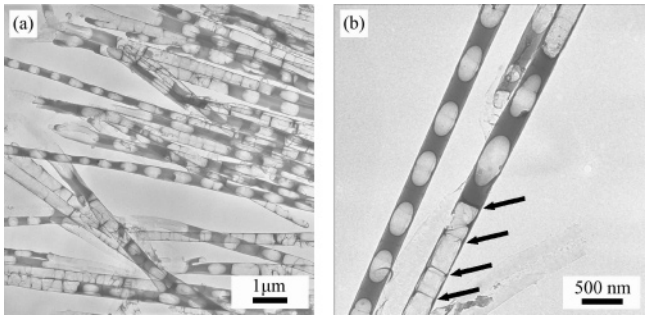

Figure 5. TEM images of carbon nanotubes (CNT)/PMMA nanorods composite: (a) low magnification image of CNT/PMMA composite; (b) high magnification image of CNT/PMMA composite. Arrows in part b show the ribs of CNT.

cavities along the length of the rod with lower and higher magnification, respectively.

Different annealing temperatures and times were used to investigate the dynamics of the structural transformation resulting from the Rayleigh instabilities. AAO membranes containing pores coated with PMMA were heated to temperatures ranging from 150 to 200 °C under vacuum for different periods of time. The structure transformation was found to occur more rapidly with lower melt viscosity, i.e., at higher temperatures, as would be expected based on the theory of Rayleigh instabilities. It was predicted that the characteristic time (τ_M) for the fastest growing mode of a thin liquid film in a capillary is[13]

$$\tau_M = \frac{12\eta b^4}{\gamma e^3} \quad (1)$$

where η is the viscosity, b is the pore radius, γ is surface tension of liquid, and e is the initial film thickness. Although this equation is derived assuming a very small film thickness compared to the size of the capillary ($e \ll b$), τ_M was found to be proportional to the viscosity of liquid. Thus, τ_M should decrease with increasing annealing temperature, as we

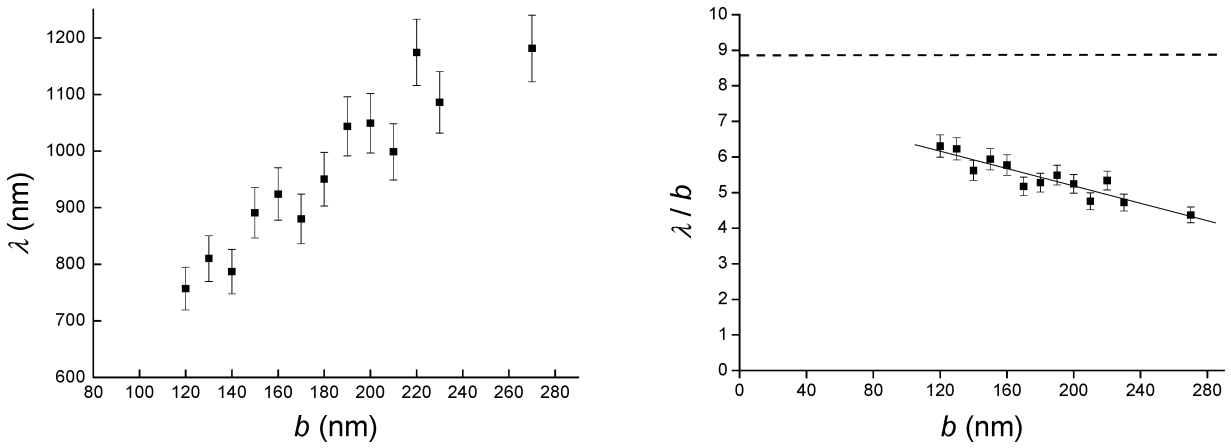

Figure 6. (a) Plot of the wavelength (λ, distance between adjacent encapsulated holes) vs the radius of the capillary, b. (b) Plot of the ratio of wavelength to the radius (λ/b) vs the radius of the capillary. The error bars are statistical errors with 95% confidence limit. The dashed line indicates the ratio of 8.89.

observed. At the annealing temperature of 200 °C, some intermediate structures can be quenched and captured within a relatively short annealing time. In Figure 3a (10 min annealing), some PMMA nanotubes completely transformed to the hole-containing nanorods while part of one tube still showed only waviness. The wave-like shape is the signature of the initial undulation of the structures. The wavelength established is maintained during the growth of the fluctuations and ultimately dictates the spacing between the adjacent holes. Figure 3b shows the wavy structure with the wavelength of $\sim$ 730 nm, which is the same as the spacing between adjacent holes in the part where a capillary bridge was found. Figure 3c shows the TEM image of hole-containing PMMA nanorods resulting from the annealing of PMMA nanotubes at 200 °C for 20 min. These structures are very similar to the structures obtained after annealing at 150 °C after 8 h. The depression and the existence of open holes on the annular thin films surrounding the periodic cavities (as can be seen in Figure 3d) may arise from damage of the electron beam.

From the time-dependent electron microscopy observations, a mechanism for the structure transformation induced by Rayleigh instabilities can be determined and is schematized in Figure 4. Initially, the PMMA nanotubes were prepared by filling the cylindrical nanopores in an AAO membrane with polymer solution followed by solvent evaporation. Upon heating to temperatures above the glass transition temperature of PMMA, undulations form on the surface of the polymer film, resulting in wave-like structures (Figure 3b) that are, due to Rayleigh instabilities, driven by the reduction in surface area or total surface energy. With time the wave grows in amplitude and, eventually the crests of the wave merge and form capillary bridges, resulting in the formation of nanorods with periodic encapsulated pores.

The films surrounding the encapsulated holes within the resultant nanorods are very thin and susceptible to being broken after removal of the template (AAO membrane), as shown in some electron microscopy images (Figures 2 and 3). Consequently, experiments were performed to enhance the stability of these unusual nanorods while maintaining the ability to perform the electron microscopy experiments for characterization. To this end, experiments were performed using amorphous carbon nanotubes (CNTs) as the template to prepare PMMA nanotubes and examine Rayleigh instabilities.

The preparation of CNTs within an AAO membrane has been described in our previous paper in detail.[21] Briefly, solutions of poly(acrylonitrile) (PAN) in dimethylformamide were drawn into the nanoporous AAO membranes by capillary force. Upon solvent evaporation, a PAN film was left on the wall of cylindrical nanopores in an AAO membrane. After stabilization at 250 °C and subsequent pyrolysis at 600 °C, PAN was converted to amorphous carbon, forming amorphous carbon nanotubes in the AAO membrane. This modified membrane was then used as a template to prepare PMMA nanotubes, forming a composite AAO/CNT/PMMA structure as described in Supporting Information. Parts a and b of Figure 5 show the CNT/PMMA nanocomposite after annealing at 150 °C for 12 h, where the AAO was removed by a weak base. As can be seen, the periodic array of pores encapsulated in PMMA nanorods is clearly observed. In some of the CNTs (Figure 5b), ribs can be seen that formed during the preparation of CNTs.[21] Nonetheless, the unique structure of the PMMA nanorods is retained and, when the PMMA nanorods are surrounded by the thin amorphous carbon nanotube, the PMMA nanorods are very robust.

The relationship between the wavelength (i.e., the spacing between the adjacent encapsulated holes) and the radius of the capillary was examined. For a thin liquid film inside a capillary of radius b, the wavelength is

$$\lambda = 2\pi\sqrt{2}b \tag{2}$$

Equation 2 assumes that the original film thickness is much thinner than the radius of the capillary and that long-range forces can be ignored.[11] In this case, the ratio between the wavelength and the radius of the capillary, λ/b, should be a constant (8.89) and independent of the size of the capillary. Figure 6a shows the plot of the wavelength vs the radius of

the capillary based on our experimental results. We can see that the wavelength increases with the radius of the capillary, however, λ/b is not constant (Figure 6b). It decreases from 6.5 to 4.5 when the radius of the capillary increases from 120 to 270 nm. This discrepancy is caused by two factors: (1) compared to the radius of the capillary, the thickness of the original film cannot be neglected; and (2) the original film thickness is thinner than 100 nm, and long-range forces may need to be considered.[10] Therefore, a different equation that considers these two factors should be able to explain the smaller ratios of the wavelength to the radius of the capillary.

In conclusion, thin films of PMMA confined within nanoscopic cylindrical pores of an AAO membrane were used to study Rayleigh instabilities. Upon heating to the melt state, the surface of PMMA nanotubes started to undulate to reduce the surface area. With time the surface undulation grew in amplitude and eventually the crests merged forming capillary bridges along with periodic encapsulated pores. The resultant hole-containing nanorods can be made mechanically robust by using amorphous carbon nanotubes as templates.

This study demonstrates a simple way to generate nanostructures that are not accessible by other experimental methods. Routes are currently being pursued to fill the pores within the nanorods with functional materials with the intent of developing novel structures for subsequent delivery applications.[23,24]

Acknowledgment. This work was supported by the U.S. Department of Energy, Office of Basic Energy Science under DEFG02-96ER45612.

Supporting Information Available: Text giving detailed experimental procedures for the sample preparation and characterization. This material is available free of charge via the Internet at http://pubs.acs.org.

References

(1) Xia, Y. N.; Yang, P. D.; Sun, Y. G.; Wu, Y. Y.; Mayers, B.; Gates, B.; Yin, Y. D.; Kim, F.; Yan, Y. Q. *Adv. Mater.* **2003**, *15*, 353.
(2) Cui, Y.; Wei, Q. Q.; Park, H. K.; Lieber, C. M. *Science* **2001**, *293*, 1289.
(3) Thess, A.; Lee, R.; Nikolaev, P.; Dai, H. J.; Petit, P.; Robert, J.; Xu, C. H.; Lee, Y. H.; Kim, S. G.; Rinzler, A. G.; Colbert, D. T.; Scuseria, G. E.; Tomanek, D.; Fischer, J. E.; Smalley, R. E. *Science* **1996**, *273*, 483.
(4) Huynh, W. U.; Dittmer, J. J.; Alivisatos, A. P. *Science* **2002**, *295*, 2425.
(5) Gleiter, H. *Acta Mater.* **2000**, *48*, 1.
(6) Steinhogl, W.; Schindler, G.; Steinlesberger, G.; Engelhardt, M. *Phys. Rev. B* **2002**, *66*, 075414.
(7) Toimil-Molares, M. E.; Balogh, A. G.; Cornelius, T. W.; Neumann, R.; Trautmann, C. *Appl. Phys. Lett.* **2004**, *85*, 5337.
(8) Plateau, J. *Transl. Annu. Rep. Smithsonian Inst.* **1873**, 1863.
(9) Rayleigh, L. *Proc. London Math. Soc.* **1878**, *10*, 4.
(10) Quere, D.; Dimeglio, J. M.; Brochard-Wyart, F. *Science* **1990**, *249*, 1256.
(11) de Gennes, P. G.; Brochard-Wyart, F.; Quere, D. *Capillarity and Wetting Phenomena*; Springer, New York, 2004.
(12) Dimeglio, J. M.; Quere, D.; Brochard-Wyart, F. *C. R. Acad. Sci.* **1989**, *309*, 19.
(13) Callegari, G.; Calvo, A.; Hulin, J. P.; Brochard-Wyart, F. *Langmuir* **2002**, *18*, 4795.
(14) Callegari, G.; Calvo, A.; Hulin, J. P. *Eur. Phys. J. E* **2005**, *16*, 283.
(15) Dersch, R.; Steinhart, M.; Boudriot, U.; Greiner, A.; Wendorff, J. H. *Polym. Adv. Technol.* **2005**, *16*, 276.
(16) Martin, C. R. *Science* **1994**, *266*, 1961.
(17) Steinhart, M.; Wendorff, J. H.; Greiner, A.; Wehrspohn, R. B.; Nielsch, K.; Schilling, J.; Choi, J.; Gösele, U. *Science* **2002**, *296*, 1997.
(18) Masuda, H.; Fukuda, K. *Science* **1995**, *268*, 1466.
(19) Li, A. P.; Müller, F.; Birner, A.; Nielsch, K.; Gösele, U. *J. Appl. Phys.* **1998**, *84*, 6023.
(20) Cepak, V. M.; Martin, C. R. *Chem. Mater.* **1999**, *11*, 1363.
(21) Chen, J. T.; Shin, K.; Leiston-Belanger, J. M.; Zhang, M. F.; Russell, T. P. *Adv. Funct. Mater.* **2006**, *16*, 1476.
(22) Zhang, M. F.; Dobriyal, P.; Chen, J. T.; Russell, T. P.; Olmo, J.; Merry, A. *Nano Lett.* **2006**, *6*, 1075.
(23) Langer, R. *Science* **1990**, *249*, 1527.
(24) Martin, C. R.; Kohli, P. *Nat. Rev. Drug Disc.* **2003**, *2*, 29.

NL0621241